Theor Chem Acc (2014) 133:1535
DOI 10.1007/s00214-014-1535-0

REGULAR ARTICLE

Transition between direct gap and indirect gap in two dimensional hydrogenated honeycomb Si_xGe_{1-x} alloys

Nan Xia · Lan-Feng Yuan · Jinlong Yang

Received: 24 April 2014 / Accepted: 1 July 2014 / Published online: 12 August 2014

Abstract Using first-principles calculations, we have explored the structural and electronic properties of fully hydrogenated honeycomb $Si_xGe_{1-x}H$ alloys. Finite band gaps are opened by hydrogenation for x in the whole range from 0 to 1, while their nature and values can be tuned by x. When x is <0.7, the band gap is direct (from Γ to Γ). And when x is ≥0.7, the gap turns into indirect (from Γ to M). For all the computed compositions, the two kinds of energy differences between valence band and conduction band, Γ–Γ and Γ–M, are described well by two polynomial functions of x. The smaller of the two functions gives a good prediction for the overall band gap at any x. The two curves cross at $x = 0.7$, leading to the change of band gap type. At PBE level, the values of band gap for different x spread from 1.09 to 2.29 eV. These findings give a new route to tune the electronic properties of these materials and may have potential applications in nanoscale optoelectronics.

Keywords Hydrogenated Si_xGe_{1-x} alloys · Virtual crystal approximation · Band gap engineering · First-principles calculation

Dedicated to Professor Guosen Yan and published as part of the special collection of articles celebrating his 85th birthday.

N. Xia · L.-F. Yuan (✉) · J. Yang (✉)
Hefei National Laboratory for Physical Sciences at Microscale, University of Science and Technology of China, Hefei 230026, China
e-mail: yuanlf@ustc.edu.cn

J. Yang
e-mail: jlyang@ustc.edu.cn

1 Introduction

With the extensive applications of graphene in the electronic industry, in the past a few years more and more attentions have been paid to two dimensional (2D) atomically thin sheets, such as boron nitride (h-BN), transition metal dichalcogenides (e.g., MoS_2 and WS_2), and hybridized $B_xC_yN_z$ [1]. Similar to graphene, these 2D structures possess fantastic properties in various aspects (electronical, magnetical, optical, and mechanical, etc.) and exhibit great application prospects [2–4]. Silicene and germanene have been widely studied experimentally and theoretically [5–7], and it has been mentioned repeatedly that their band structures show linear band crossing at the Fermi level, and thus, the charge carriers behave like a massless Dirac fermion [8], similar to the case of graphene [9].

As two most important materials in the semiconductor industry, Si and Ge are both group 14 elements with similar structural properties; therefore, they can randomly mix to form alloys [10]. It has also been demonstrated that bulk Si_xGe_{1-x} alloys can be fabricated on Si substrates [11]. Not long ago, Padilha et al. [12] suggested that the electronic properties of Si_xGe_{1-x} random alloys in the honeycomb monolayer structure can be tuned by the value of x. To open a band gap and regulate the electronic properties of graphene-like materials, a variety of methods have been put forward, such as applying an external electric field [13], introducing hydrogen vacancies [14], uniaxial compression [15], biaxial compressive strain [16], cutting 2D materials into nanoribbons [17], and stacking into bilayer structures [18]. For silicene and germanene, hydrogenation is predicted to be a viable mean to open a finite gap [19, 20]. Therefore, it is highly probable that the 2D hydrogenated Si_xGe_{1-x} alloys also have finite gaps. If this is so, then we get a new parameter to manipulate this gap, i.e., the alloy

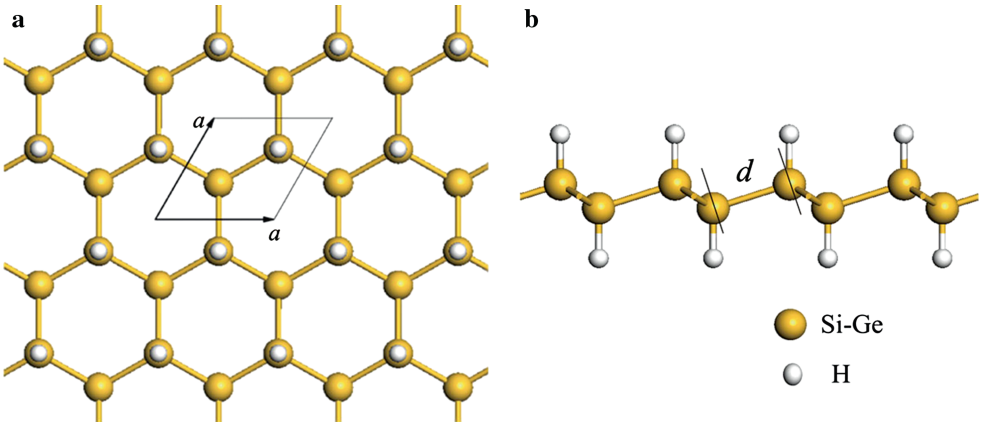

Fig. 1 Structures of $Si_xGe_{1-x}H$ alloys from the top view (**a**) and from the side view (**b**). The *yellow* and *white spheres* refer to the hybrid Si–Ge atoms and hydrogen atoms, respectively. The rhombus is a unit cell

composition (x). In order to explore this route, we hereby investigate the evolution of the band structures of 2D disordered fully hydrogenated Si_xGe_{1-x} alloys (denoted as $Si_xGe_{1-x}H$), via first-principles calculations.

2 Methods and computational details

Our ab initio calculations are based on density functional theory (DFT) [21, 22] and are performed by the CASTEP software [23]. The generalized gradient approximation (GGA) with the Perdew–Burke–Ernzerholf (PBE) functional [24] is selected as the exchange correlation potential. For all the calculations, the ultrasoft pseudopotentials are used, with a 600 eV cutoff energy for the plane-wave basis. Both the lattice constants and the atomic positions are fully relaxed. The tolerances for geometry optimizations are 1.0×10^{-5} eV/atom for total energy, 0.02 eV/Å for maximum Hellman–Feynman forces, 0.1 GPa for maximum stress, and 0.002 Å for maximum ionic displacement. The periodic boundary condition is applied in the normal direction of the monolayer, with vacuum space of 20 Å to minimize the interlayer interaction. A primitive cell containing two Si (Ge) atoms and two H atoms is used, as shown in Fig. 1. Following the Monkhorst–Pack scheme [25], Brillouin zone integration is carried out at $9 \times 9 \times 1$ k-points for the geometry optimization and $15 \times 15 \times 1$ k-points for the static total energy calculations.

To simulate the electronic structure of these disordered alloys, the virtual crystal approximation (VCA) is used, which is a simple and reasonable approximation for this task. In this approximation, one studies a crystal with the primitive periodicity, but composed of fictitious atoms, which are hybrids of two or more element types [26]. The meaning of "hybrid" is that the potential of a virtual atom is treated as the concentration-weighted average of the constituent potentials, neglecting further compositional disorder effects [27]. VCA is widely used in the literature. For example, Bellaiche et al. [26] successfully employed VCA to study the dielectric and piezoelectric properties of the $Pb(Zr_{0.5}Ti_{0.5})O_3$ perovskite solid solution in its paraelectric and ferroelectric phases. Winkler et al. [28] showed that the VCA approach can be used to study Al/Si disorder in silicates, reproducing the experimental structural parameters.

Employing VCA, a series of $Si_xGe_{1-x}H$ alloys with eleven different compositions have been simulated. The choices for x are from 0 (hydrogenated germanene) to 1 (hydrogenated silicene), with increment of 0.1, in the hope that the properties of an alloy with any x can be roughly estimated based on these eleven data points. There are two common configurations of fully hydrogenated silicene (germanene), i.e., boat like and chair like. It was reported that the chair configurations of silicene and germanene are more stable than the boat ones, by about 10 meV/atom [29]. In our calculations, for three typical alloys ($x = 0.3$, 0.5, and 0.8), the chair configurations are more stable than the boat ones as well, with the energy differences being 12.8, 12.8, and 13.9 meV/atom, respectively. Consequently, we will only consider the chair configurations of $Si_xGe_{1-x}H$ alloys afterward.

3 Results and discussions

After geometry optimizations, the calculated lattice parameters a and atom bond lengths d of hydrogenated silicene and germanene are 3.88, 2.35, and 4.06, 2.45 Å respectively, which are consistent with the previous theoretical results 3.884, 2.356 Å [30] and 4.06, 2.46 Å [19]. Upon hydrogenation, the calculated buckling heights h are 0.72 and 0.75 Å, distinctly larger than those of silicene (0.45 Å) and germanene (0.64 Å). Namely, the hydrogenated configurations are more tortuous than the pristine structures. This can be understood in terms of variation in hybridization state along with hydrogenation. In silicene (germanene), the buckled structure gives rise to reduced π–π

Table 1 Structural and electronic parameters of $Si_xGe_{1-x}H$ alloys in different composition of Si element (x)

x	a (Å)	Φ (eV)	$E_{\Gamma-\Gamma}$ (eV) (direct)	$E_{\Gamma-M}$ (eV) (indirect)
0	4.058	4.809	1.089	1.912
0.1	4.046	4.855	1.435	2.035
0.2	4.035	4.870	1.710	2.135
0.3	4.023	4.972	1.905	2.207
0.4	4.009	4.932	2.058	2.250
0.5	3.998	4.950	2.157	2.271
0.6	3.983	4.992	2.234	2.285
0.7	3.962	5.015	2.297	2.285
0.8	3.941	5.028	2.327	2.262
0.9	3.915	5.012	2.340	2.224
1	3.884	5.029	2.332	2.174

The entries a, Φ, $E_{\Gamma-\Gamma}$, and $E_{\Gamma-M}$ are the lattice constant, the effective work function, the gaps between conduction band and valence band from Γ to Γ and from Γ to M, respectively

overlap between p_z orbitals of adjacent Si (Ge) atoms, so the hybridization of each Si (Ge) atom is intermediate between sp^2 and sp^3. After new σ bonds are formed with H atoms, the Si–Ge atoms in $Si_xGe_{1-x}H$ become purely sp^3 hybridized. Therefore, the bond angles in $Si_xGe_{1-x}H$ are greater than those in silicene and germanene, resulting in higher degree of buckling.

For all the eleven compositions, the lattice parameters, the effective work functions (Φ), and two kinds of energy differences between valence band and conduction band (Γ–Γ and Γ–M) are listed in Table 1. The lattice parameter a decreases monotonically from 4.058 to 3.884 Å as x increases from 0 to 1, which is naturally owing to the larger atomic radius of Ge than that of Si. The effective work function, defined as the difference in potential energy of one electron between the highest occupied molecular orbital (HOMO) and the vacuum level, ranges from 4.81 to 5.03 eV.

To further illustrate how the composition affects the electronic properties of $Si_xGe_{1-x}H$, the band structures of four typical systems are presented in Fig. 2. In silicene and germanene, the π and π* bands cross at the k-point around the Fermi level, rendering them gapless. On the other hand, all the 2D $Si_xGe_{1-x}H$ alloys have finite band gaps, basically due to the interaction between the p_z orbitals of Si (Ge) and the 1 s orbitals of H atom. The valence band maximum (VBM) is always located at the Γ point. However, the conduction band minimum (CBM) can be either in Γ or in M, depending on the composition. Therefore, hydrogenated silicene is an indirect band gap (2.17 eV) semiconductor, while hydrogenated germanene is a direct band gap (1.09 eV) semiconductor. These results are qualitatively and quantitatively consistent with previous computational

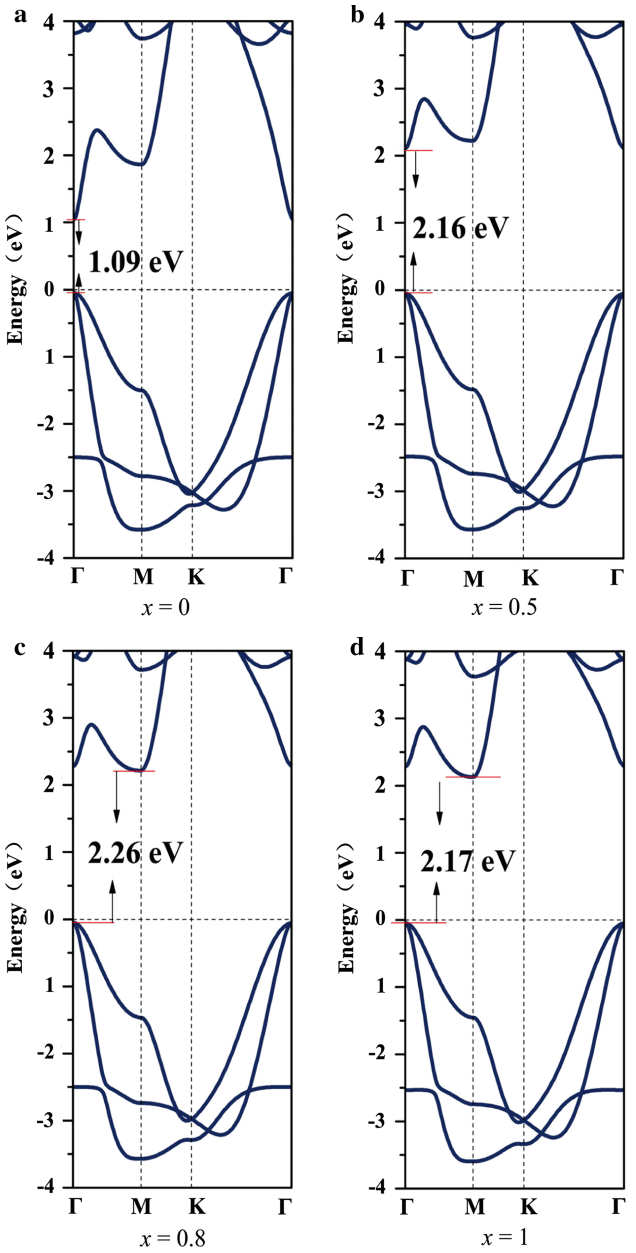

Fig. 2 Band structures of $Si_xGe_{1-x}H$ alloys with four kinds of composition, i.e. $x = 0$ (**a**), 0.5 (**b**), 0.8 (**c**), 1 (**d**). The band gaps are noted in the picture. The Fermi levels are set to be energy zero

results, for instance, 2.0 eV [29], 2.19 eV [19] and 2.21 eV [14] for hydrogenated silicene, and 0.94 eV [19], 1.4 eV [29] and 1.5 eV [20] for hydrogenated germanene. Among the band gaps of our 11 systems, that of $Si_{0.7}Ge_{0.3}H$ is found to be the biggest, which is an indirect gap of 2.29 eV, while the gap of hydrogenated germanene (1.09 eV) is the smallest. Thus, the band gap of hydrogenated $Si_xGe_{1-x}H$ alloys can be tuned in the range from 1.09 to 2.29 eV by changing the composition. This is reminiscent of the result of Gao et al. [31] that the band gap of hydrogenated

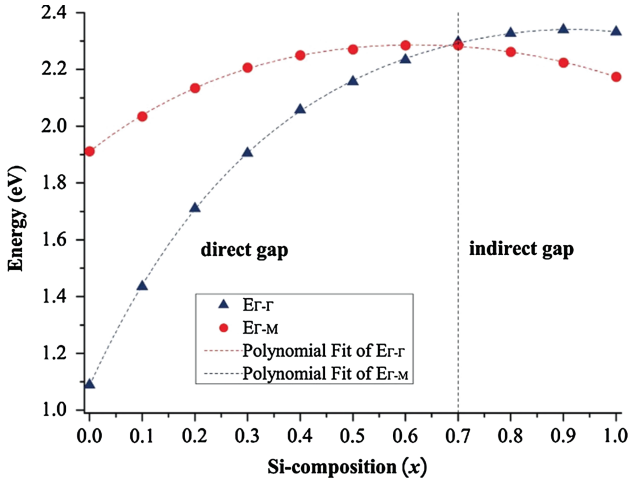

Fig. 3 Two sets of energy differences between valence and conduction bands of $Si_xGe_{1-x}H$ as functions of Si composition (x): Γ–Γ (*triangle dots*) and Γ–M (*round dots*). The corresponding fourth order polynomial fitting curves are displayed as the *dash lines*

graphene can be continuously tuned by H coverage and configuration from 0 to 4.66 eV. That is a tuning in a wider range and with a constant nature of gap (direct), while our result is a tuning in a narrower range and with a variable nature of gap (from direct to indirect).

To gain further understanding on the transition of gap type, we list the Γ–Γ and Γ–M energy differences between valence band and conduction band for each composition in Table 1. We fit the two sets of data by two polynomial functions and find that fourth order polynomials are required to gain satisfactory match, as shown in Fig. 3. The curve for the Γ–Γ gap starts from the lowest value (1.089 eV) at $x = 0$ and increases quickly with x. When x approaches 1, this curve becomes flat. It reaches a maximum (2.340 eV) at $x = 0.9$ and drops a little bit (2.332 eV) eventually at $x = 1$. On the other hand, the curve for the Γ–M gap spreads in a much narrower range, from 1.912 to 2.285 eV. The maximum is reached at $x = 0.6$ and 0.7. In the beginning, i.e., for small values of x, the Γ–Γ gap is less than the Γ–M gap, so the system is a direct gap semiconductor. The two curves cross roughly at $x = 0.7$. After that, the order between the two gaps is reversed, and the system becomes an indirect gap semiconductor. Therefore, the band gap of any alloy can be represented by the smaller of the two polynomial functions, as listed below (in eV):

$$Eg = \begin{cases} 1.087 + 4.029x - 5.383x^2 + 3.875x^3 - 1.276x^4 (0 \le x < 7) \\ 1.911 + 1.465x - 1.948x^2 + 1.171x^3 - 0.425x^4 (0.7 \le x \le 1) \end{cases}$$

Using this piecewise function, one can describe well the band gap of $Si_xGe_{1-x}H$ for x along the whole range from 0 to 1.

At last, let us discuss the numerical uncertainty of our calculated gaps. There are two levels of errors, one from the treatment to disorder (i.e., VCA) and the other from the selection of functional (i.e., PBE). To check the viability of VCA in our systems, we compare the electronic properties by VCA and by conventional ordered PBE calculations for $Si_{0.5}Ge_{0.5}H$. We employ 6 kinds of supercells, i.e., $n \times n$ for $n = 1$–6, with different atomic arrangements of Si and Ge to simulate the randomized alloy. We test 8 arrangements for the 4×4 supercell and one arrangement for each of the other supercells. All the VCA and PBE calculations give rise to direct gaps. The band gaps from the supercell calculations are in the range of 1.68–1.72 eV, about 80 % of the VCA value 2.157 eV. Taking into consideration that a more realistic representation of the random alloy would require much larger supercells and many more atomic arrangements, this degree of agreement is acceptable. We acknowledge that VCA is a simple model, and the huge saving in computational cost is a major advantage and the main reason for us to adopt this method.

As for the second factor, GGA is known to tend to underestimate the band gaps of semiconductors and insulators and gives values typically 50–60 % smaller than those from better hybrid DFT methods. The gaps of fully hydrogenated silicene and germanene by HSE06 are reported to be 3.51 eV [32] and 1.56 eV [33], respectively. The optical properties of hydrogenated germanene were investigated by diffuse reflectance absorption (DRA) spectroscopy, and a linear approximation of the absorption edge suggests a band gap of approximately 1.59 eV [33]. There is no experimental data concerning the electronic properties of hydrogenated silicene. Therefore, the scaling factor for band gaps can be estimated as the ratio between the HSE06 to PBE values, which is 1.618 for hydrogenated silicene and 1.431 for hydrogenated germanene. So to compare quantitatively with experiments, it will be advisable to scale our PBE gaps by similar ratios, giving a range of 1.56–3.70 eV.

4 Conclusions

In summary, first-principles calculations based on the VCA have been applied to investigate the structural and electronic structures of 2D hydrogenated Si_xGe_{1-x} alloys. At PBE level, the band gap of these systems can be tuned in a range of 1.09–2.29 eV via varying their compositions. For $x < 0.7$, the alloys are direct band gap (Γ–Γ) semiconductors. And after x reaches 0.7, the band gaps transform to indirect (Γ–M). The origin of this transition is the change of the CBM location from Γ to M, or in another word, the crossing of the two curves of the Γ–Γ and Γ–M energy differences versus x. We fit the two curves by two polynomials, thus giving a tool to predict the band gap in the whole

range in terms of a piecewise function. Around the transition composition ($x = 0.7$), a small change in composition can lead to qualitative change in electronic and photonic properties for these alloys. Therefore, once combined with advanced Si/Ge nanotechnology, these materials have very valuable potential for band engineering and optical application.

Acknowledgments This work is partially supported by the National Key Basic Research Program (Contract No. 2011CB921404), by NSFC (Contract Nos. 21121003, 91021004, 21233007, 21222304), by CAS (Contract Nos. XDB01020300, XDB10030402), and by USTCSCC, SCCAS, Tianjin, and Shanghai Supercomputer Centers.

References

1. Song X, Hu J, Zeng H (2013) J Mater Chem C 1:2952
2. Santos EJG (2013) J Phys Chem C 117:6420
3. Yan JA, Stein R, Schaefer DM, Wang XQ, Chou MY (2013) Phys Rev B 88:121403
4. Wu IJ, Guo GY (2007) Phys Rev B 76:035343
5. Fleurence A, Friedlein R, Ozaki T, Kawai H, Wang Y, Yamada-Takamura Y (2012) Phys Rev Lett 108:245501
6. Feng B, Ding Z, Meng S, Yao Y, He X, Cheng P, Chen L, Wu K (2012) Nano Lett 12:3507
7. Zheng F, Zhang C (2012) Nanoscale Res Lett 7:1
8. Liu CC, Feng W, Yao Y (2011) Phys Rev Lett 107:076802
9. Novoselov KSA, Geim AK, Morozov SV, Jiang D, Katsnelson M, Grigorieva I, Dubonos S, Firsov A (2005) Nature 438:197
10. Lang DV, People R, Bean JC, Sergent AM (1985) Appl Phys Lett 47:1333
11. Bean JC, Feldman LC, Fiory AT, Nakahara ST, Robinson IK (1984) J Vac Sci Technol A 2:436
12. Padilha JE, Seixas L, Pontes RB, da Silva AJ, Fazzio A (2013) Phys Rev B 88:201106
13. Drummond ND, Zolyomi V, Fal'Ko VI (2012) Phys Rev B 85:075423
14. Pan L, Liu HJ, Wen YW, Tan XJ, Lv HY, Shi J, Tang XF (2012) Appl Surf Sci 258:10135
15. Kaltsas D, Tsatsoulis T, Ziogos OG, Tsetseris L (2013) J Chem Phys 139:124709
16. Houssa M, Pourtois G, Afanas'ev VV, Stesmans A (2010) Appl Phys Lett 96:082111
17. Topsakal M, Ciraci S (2010) Phys Rev B 81:024107
18. Min H, Sahu B, Banerjee SK, MacDonald AH (2007) Phys Rev B 75:155115
19. Wei W, Dai Y, Huang B, Jacob T (2013) Phys Chem Chem Phys 15:8789
20. Voon LCLY, Sandberg E, Aga RS, Farajian AA (2010) Appl Phys Lett 97:163114
21. Hohenberg P, Kohn W (1964) Phys Rev 136:B864
22. Kohn W, Sham LJ (1965) Phys Rev 140:A1133
23. Segall MD, Lindan PJD, Probert MJ, Pickard CJ, Hasnip PJ, Clark SJ, Payne MC (2002) J Phys Condens Matter 14:2717
24. Perdew JP, Burke K, Ernzerhof M (1996) Phys Rev Lett 77:3865
25. Monkhorst HJ, Pack JD (1976) Phys Rev B 13:5188
26. Bellaiche L, Vanderbilt D (2000) Phys Rev B 61:7877
27. Bechiri A, Benmakhlouf F, Bouarissa N (2003) Mater Chem Phys 77:507
28. Winkler B, Pickard C, Milman V (2002) Chem Phys Lett 362:266
29. Houssa M, Scalise E, Sankaran K, Pourtois, G, Afanas'ev VV, Stesmans A (2011) Appl Phys Lett 98:223107
30. Wang XQ, Li HD, Wang JT (2012) Phys Chem Chem Phys 14:3031
31. Gao H, Wang L, Zhao J, Ding F, Lu J (2011) J Phys Chem C 115:3236
32. Zhang P, Li XD, Hu CH, Wu SQ, Zhu ZZ (2012) Phys Lett A376:1230
33. Bianco E, Butler S, Jiang S, Restrepo OD, Windl W, Goldberger JE (2013) ACS Nano 7:4414

http://www.springer.com/978-3-662-47844-8

Guosen Yan

A Festschrift from Theoretical Chemistry Accounts

Guo, H.; Xie, D.; Yang, W. (Eds.)

2015, VI, 209 p. 133 illus., 99 illus. in color., Hardcover

ISBN: 978-3-662-47844-8